Received: 10 April 2019 | Revised: 4 September 2019 | Accepted: 21 October 2019

DOI: 10.1002/bit.27213

BIOTECHNOLOGY BIOENGINEERING WILEY

ARTICLE

Targeted capture of Chinese hamster ovary host cell proteins: Peptide ligand binding by proteomic analysis

R. Ashton Lavoie[1] | Alice di Fazio[1] | Taufika Islam Williams[2] | Ruben Carbonell[1,3,4] | Stefano Menegatti[1,3]

[1]Department of Chemical and Biomolecular Engineering, North Carolina State University, Raleigh, North Carolina

[2]Molecular Education, Technology, and Research Innovation Center (METRIC), North Carolina State University, Raleigh, North Carolina

[3]Biomanufacturing Training and Education Center (BTEC), North Carolina State University, Raleigh, North Carolina

[4]The National Institute for Innovation in Manufacturing Biopharmaceuticals (NIIMBL), Newark, Delaware

Correspondence
Ruben Carbonell and Stefano Menegatti, Department of Chemical and Biomolecular Engineering, North Carolina State University, Centennial Campus, 911 Partners Way, Engineering Building I (EB1), Raleigh, NC 27695-7905.
Email: ruben@ncsu.edu and smenega@ncsu.edu

Funding information
Kenan Institute for Engineering, Technology and Science

Abstract

The clearance of host cell proteins (HCPs) is of crucial importance in biomanufacturing, given their diversity in composition, structure, abundance, and occasional structural homology with the product. The current approach to HCP clearance in the manufacturing of monoclonal antibodies (mAbs) relies on product capture with Protein A followed by removal of residual HCPs in flow-through mode using ion exchange or mixed-mode chromatography. Recent studies have highlighted the presence of "problematic HCP" species, which are either difficult to remove (Group I), can degrade the mAb product (Group II), or trigger immunogenic reactions (Group III). To improve the clearance of these species, we developed a family of synthetic peptides that target HCPs and exhibit low binding to IgG product. In this study, these peptides were conjugated onto chromatographic resins and evaluated in terms of HCP clearance and mAb yield, using an industrial mAb-producing CHO harvest as model supernatant. To gather detailed knowledge on the binding of individual HCPs, the unbound fractions were subjected to shotgun proteomic analysis by mass spectrometry. It was found that these peptide ligands exhibit superior HCP binding capability compared to those of the benchmark commercial resins commonly used in mAb purification. In addition, some peptide-based resins resulted in much lower losses of product yield compared to these commercial supports. The proteomic analysis showed effective capture of many "problematic HCPs" by the peptide ligands, especially some that are weakly bound by commercial media. Collectively, these results indicate that these peptides show great promise toward the development of next-generation adsorbents for safer and cost-effective manufacturing of biologics.

KEYWORDS
host cell proteins, monoclonal antibodies, polishing, peptide ligands, protein purification

1 | INTRODUCTION

Recent advances in monitoring and control capabilities in biopharmaceutical manufacturing are reshaping our understanding of the production processes. The manufacture of monoclonal antibodies (mAbs) in particular, owing to its reliance on widely used platform processes, has enabled a more detailed understanding of the process parameters that determine more robust processes and safer

Abbreviations: CHO, Chinese hamster ovary cell line; DIPEA, diisopropylethylamine; DMF, N, N′-dimethylformamide; EDT, ethanedithiol; ESI, electrospray ionization; FASP, filter-aided sample preparation; Fmoc, fluorenylmethyloxycarbonyl; FT, flow-through; HATU, Hexafluorophosphate Azabenzotriazole Tetramethyl Uronium; HCP, host cell protein; IgG, immunoglobulin G; mAb, monoclonal antibody; nano-LC-MS/MS, nano liquid chromatography coupled to tandem mass spectrometry; NMP, N-methyl-2-pyrrolidone; NSAF, normalized spectral abundance factor; SpC, spectral count; SPPS, solid phase peptide synthesis; TFA, trifluoroacetic acid; TIPS, triisopropylsilane; UPLC, ultra performance liquid chromatography.

products. The application of proteomics-based approaches at different stages of mAb production has revealed new challenges related to the removal of the host cell protein (HCP) impurities secreted by the mAb-expressing cells. In a recent review of HCP removal strategies, Goey, Al huthali, and Kontoravdi (2018) presented a thorough survey of HCPs that pose a significant risk to patient's health, and highlighted the challenges that mAb manufacturers face in ensuring rigorous HCP clearance. The authors recommend that upstream process conditions be controlled to minimize downstream bottlenecks and challenges, including high product titers as well as high HCP levels that accompany them. The importance of this approach was also highlighted by Lee and coworkers, who showed that the HCP content can be reduced at the start through the development of HCP-knockout cell lines (Chiu et al., 2017), and the optimization of cell culture parameters, such as cell age and cell viability, to minimize HCP levels (Park et al., 2017; Valente, Lenhoff, & Lee, 2015). Complementary to these approaches in upstream processing is the effort toward improving the downstream capture of HCPs by developing robust purification processes that are tolerant to the inherent variability in cell culture. In this regard, much attention has recently been focused on "problematic" HCPs, that is, proteins that (a) co-elute with mAbs at the Protein A capture step (Gagnon et al., 2014; Gan et al., 2013; Hogwood, Tait, Koloteva-Levine, Bracewell, & Smales, 2013; Zhang et al., 2014) or associate with most mAbs (Aboulaich et al., 2014; Gagnon et al., 2014; Levy, Valente, Choe, Lee, & Lenhoff, 2014; Mechetner, Sood, Nguyen, Gagnon, & Parseghian, 2011), (b) cause degradation of the product of interest through enzymatic digestion (Bee et al., 2015) or degradation of the excipients during storage (Chiu et al., 2017), or (c) present high immunogenicity risk at trace concentrations (Bailey-Kellogg et al., 2014). It is important to accurately monitor the residual levels of these HCPs through the various stages of upstream and downstream processing.

This study seeks to enhance current HCP clearance strategies by identifying synthetic ligands that specifically capture HCPs commonly present in mAb-containing fluids, with particular focus on the targeting of problematic HCPs. In prior work (Lavoie et al., 2019), we described the identification of HCP-specific peptide ligands and the evaluation of their binding activity of HCPs and IgG product compared to benchmark commercial resins Capto Q (anion exchange) and Capto Adhere (mixed-mode) (Lavoie et al., 2019). These peptides include multipolar (MP) and hydrophobic/positive (HP) sequences. The former feature a combination of positively and negatively charged amino acids (Lys, Arg, His, and Asp) and a minor presence of aromatic residues (Phe and Tyr), while the later are distinctively rich in positively charged, aromatic, and aliphatic (Ala and Ile) residues. In this study, we present an in-depth evaluation of binding of specific HCPs by the peptide ligands, compared to commercial ion exchange and mixed-mode media. A bottom-up proteomic analysis of the feed sample and supernatant fractions from static binding studies described in the prior work (Lavoie et al., 2019) was conducted using nano liquid chromatography coupled to tandem mass spectrometry (nano-LC–MS/MS). This methodology allowed for identification and semi-quantitative measurement of individual HCP capture by the peptide ligands. The values of bound HCPs were then be correlated with binding conditions (loading ratio and buffer composition and pH), and this enabled a determination of whether combinations of resins may be beneficial in improving HCP removal, particularly for difficult-to-clear HCPs in current mAb platform processes. Previous work by Kornecki et al. (2017) outlines the difficulty in the clearance of HCPs with existing commercial options. Therefore, this study aims to provide improved options for more selective removal of this highly diverse and complex population of contaminants.

This study focuses on problematic HCPs in three primary categories based on risk factors described above: (a) HCPs co-eluting with mAbs in the capture step, herein referred to as Group I (Aboulaich et al., 2014; Gagnon et al., 2014; Levy et al., 2014; Mechetner et al., 2011; Zhang et al., 2016), including IgG-associated and Protein A-binding HCPs, (b) HCPs that cause product degradation, or Group II (Aboulaich et al., 2014; Bee et al., 2015; Chiu et al., 2017; Goey et al., 2018; Zhang et al., 2014), and (c) HCPs with high immunogenicity risk, or Group III (Bailey-Kellogg et al., 2014; Fischer et al., 2017; Goey et al., 2018; Jawa et al., 2016). In typical mAb platform processes, the large majority of HCPs are removed at the product capture step with Protein A-based adsorbents; thus, the design of the subsequent intermediate and final polishing steps is highly dependent on their ability to remove the species that co-elute with IgG from Protein A. Numerous studies in recent years have focused on identifying the mechanism behind co-elution and selecting process conditions that prevent persistence of these species post-Protein A. For a number of species, co-elution is a result of direct association with the mAb (Aboulaich et al., 2014; Gagnon et al., 2014; Levy et al., 2014; Mechetner et al., 2011); thus, the capture of this subset of impurities without dissociation from the mAb product can result in decreased product yield, although the extent of mAb bound by these HCPs is, as of yet, debated. Novel polishing strategies that target this family of HCPs are required to lower product loss through diligent selection of wash steps or modifiers that induce dissociation if the capture of product-bound species results in substantial product loss. Outside of product-associated HCPs, species that co-elute with mAbs may result from interaction with Protein A, as it has been determined for chromatin (Gagnon et al., 2014). Chromatin has also been shown to cause co-elution of "hitchhiker" HCPs (Mechetner et al., 2011), which associates with HCPs that bind mAbs or Protein A, thus effectively behaving as co-eluting species.

Group II HCPs, or mAb-degrading HCPs, comprise enzymatically active species that induce product degradation. This study focuses on species that are known to cleave or alter the mAb product directly, including cathepsins, metalloproteinases, serine protease HTRA1, and sialidases (Aboulaich et al., 2014; Bee et al., 2015; Goey et al., 2018; Zhang et al., 2014). In addition, this group includes species that cause degradation due to conformational changes in the mAb, such as protein disulfide isomerase, 78 kDa glucose-regulated protein (also known as binding immunoglobulin protein or BiP), and heat shock

protein (Goey et al., 2018). This subset also includes species that are thought to cause product degradation indirectly; lipoprotein lipase, for example, is thought to degrade polysorbate excipients in final formulations, resulting in reduced shelf life of the drug product (Chiu et al., 2017).

Group III HCPs includes species that have a high risk of immunogenicity. Because any foreign protein can stimulate an immunogenic response, this study considered species that have been shown to stimulate an immunogenic response, such as phospholipase B-like protein (Fischer et al., 2017) and species that are indicated to have a high risk of immunogenicity based on *in silico* modeling (Bailey-Kellogg et al., 2014; Goey et al., 2018; Jawa et al., 2016).

The results of this study show efficient and selective capture of these three groups of problematic HCPs by the MP and HP peptide ligands identified in prior efforts (Lavoie et al., 2019). Furthermore, they demonstrate improved salt-tolerance of our novel ligands, enabling the development of HCP "scrubbing" applications before product capture or diafiltration steps.

2 | MATERIALS AND METHODS

2.1 | Materials

For peptide synthesis and deprotection, Toyopearl AF-Amino-650M resin for secondary screening synthesis, triisopropylsilane, and 1,2-ethanedithiol were obtained from Millipore Sigma (St. Louis, MO). N′,N′-dimethylformamide (DMF), dichloromethane, methanol, and N-methyl-2-pyrrolidone were obtained from Fisher Chemical (Hampton, NH). Fluorenylmethoxycarbonyl- (Fmoc-) protected amino acids Fmoc-Gly-OH, Fmoc-Ser(tBu)-OH, Fmoc-Ile-OH, Fmoc-Ala-OH, Fmoc-Phe-OH, Fmoc-Tyr(But)-OH, Fmoc-Asp(OtBu)-OH, Fmoc-His(Trt)-OH, Fmoc-Arg(Pbf)-OH, Fmoc-Lys(Boc)-OH, Fmoc-Asn(Trt)-OH, and Fmoc-Glu(OtBu)-OH in addition to 7-Azabenzotriazol-1-yloxy) tripyrrolidino-phosphonium hexafluorophosphate, diisopropylethylamine, piperidine, and trifluoroacetic acid were obtained from ChemImpex International (Wood Dale, IL).

For proteomic analysis, acetonitrile, urea, tris, iodoacetamine, and formic acid were obtained from Fisher Chemical (St. Louis, MO), ReproSil-Pur 120 Å C18-AQ, 3 µm resin was obtained from Dr. Maisch GmbH (Ammerbuch-Entringen, Germany), and a 25 cm × 75 µm PicoFrit analytical column was obtained from New Objective (Woburn, MA). The analytical nano-LC column was pressure-packed in-house with C18 stationary phase. Sequencing grade modified trypsin was obtained from Promega Corporation. Amicon 10-kD MWCO centrifugal filters were obtained from Millipore Sigma. Biotechnology-grade dithiothreitol was obtained from VWR.

For static binding studies, sodium chloride, sodium phosphate (dibasic), sodium hydroxide, hydrochloric acid, bis-tris, and tris were obtained from Fisher Chemical. Macrosep Advance 3 kDa MWCO Centrifugal Devices were supplied by Pall Corporation (Ann Arbor, MI). The model mAb production CHO-K1 cell culture harvest used for secondary screening was provided by Fujifilm Diosynth (RTP, NC). Capto Q and Capto Adhere chromatography resins were generously provided by GE Life Sciences (Marlborough, MA).

2.2 | Toyopearl peptide resin synthesis and deprotection

The synthesis procedure was performed according to a protocol adapted from Menegatti et al. (2016) and is described in detail in prior work (Lavoie et al., 2019). Individual ligand candidates previously identified were synthesized and pooled as described in previous work (Lavoie et al., 2019). Briefly, the peptides were individually synthesized directly on Toyopearl AF-Amino-650M resin, and the resulting adsorbents were pooled as follows: (a) hexameric hydrophobic positive (6HP) resin, comprising of the peptide sequences GSRYRYGSG, RYYYAIGSG, AAHIYYGSG, IYRIGRGSG, HSKIYKGSG; (b) hexameric multipolar (6MP) resin, comprising ADRYGHGSG, DRIYYYGSG, DKQRIIGSG, RYYDYGGSG, YRIDRYGSG; (c) tetrameric hydrophobic positive (4HP) resin, comprising HYAIGSG, FRYYGSG, HRRYGSG, RYFFGSG; and (d) tetrameric multipolar (4MP) resin, comprising DKSIGSG, DRNIGSG, HYFDGSG, and YRFDGSG. All ligands were synthesized using standard Fmoc-amino acid coupling chemistry and deprotection procedures as described in prior work (Lavoie et al., 2019). Resins were washed three to five times first with DMF then 20% methanol and stored in 20% methanol at 2–8°C.

2.3 | Static binding of HCPs to peptide and control resins

The procedure for the static binding study performed to evaluate the peptide and commercially available control resins (Capto Q and Capto Adhere) is described in detail in prior work (Lavoie et al., 2019). Briefly, a mAb production clarified cell culture harvest derived from a CHO-K1 wild-type cell line was obtained for use as feed material. Clarified cell culture harvest was concentrated by a factor of ~4 × (~1.2 mg/ml host cell protein) and diafiltered to the appropriate buffer condition using Macrosep Advance 3 kDa MWCO Centrifugal Devices. For pH 6 and 7 conditions, 10 mM Bis-Tris buffer solutions were used, and 10 mM Tris was used for pH 8 conditions, with "low" and "high" salt buffers composed of 20 mM NaCl and 150 mM NaCl, respectively. The Toyopearl-based peptide resins (6HP, 6MP, 4HP, 4MP) were tested alongside commercially available resins common in mAb purification with interaction capabilities similar to those of the peptide resins, Capto Q and Capto Adhere. The resins were aliquoted into 1 ml solid phase extraction tubes at 25 µl settled resin volume and equilibrated with 3 × 500 µl of the appropriate load buffer. Resins were then incubated with the diafiltered CHO-S harvest for 1 hr on a rotator at HCP loads of ~5 mg HCP/ml resin and the resulting supernatant was collected. The resins were then washed with 500 µl load buffer, and the supernatant samples (combination of the unbound fraction from static binding and the following wash) were pooled for analysis. No

elution was performed in this study, as the resins were employed as single-use adsorbents.

2.4 | Proteomic analysis

Supernatant samples were prepared for proteomic analysis by filter-aided sample preparation with a modified trypsin digest adapted from the method described by Wisniewski, Zougman, Nagaraj, and Mann (2009). Briefly, 30 µl load sample or 160 µl pooled static binding supernatant and wash samples were denatured in 5 mM dithiothreitol at 56°C for 30 min. The samples were then washed twice with 8 M urea, 0.1 M Tris HCl solution in 3 kDa MWCO Amicon Ultra 0.5-ml spin filters (EMD Millipore, Darmstadt, Germany). Samples were then alkylated with 0.05 M iodoacetamide at room temperature for 20 min. After washing again with 8 M urea, 0.1 M tris HCl followed by 50 mM ammonium bicarbonate, samples were trypsinized overnight at 37°C with 15 µg/ml sequencing grade modified trypsin for a targeted trypsin:protein ratio of ~1:100. Finally, samples were washed again with 50 mM ammonium bicarbonate before nano-LC-MS/MS analysis. Samples were then evaporated to dryness by speed-vac, reconstituted in 1,000 µl aqueous 2% acetonitrile, 0.1% formic acid (mobile phase A), and then further diluted 1:5 in mobile-phase A before injection.

For nano-LC-MS/MS-based proteomic analysis, all measurements were conducted at the Molecular Education, Technology, and Research Innovation Center (METRIC) at NC State University. Samples were loaded as 2-µl injections and proteins were separated by a 60 min linear gradient at 300 nl/min of mobile-phase A and mobile-phase B (0.1% formic acid in acetonitrile) from 0–40% mobile-phase B. The orbitrap was operated as follows: positive ion mode, acquisition—full scan (m/z 400–1,400) with 120,000 resolving power in MS mode, MS/MS acquisition using top 20 data-dependent acquisition (DDA) implementing higher-energy collisional dissociation with a normalized collision energy setting of 27%. Dynamic exclusion was utilized to maximize depth of proteome coverage by minimizing reinterrogation of previously sampled precursor ions.

Raw nano-LC-MS/MS data were processed using Proteome Discoverer 2.2 (Thermo Fisher Scientific, San Jose, CA). Searching was performed with a 5 ppm precursor mass tolerance and 0.02 Da fragment tolerance with the *Cricetulus griseus* (Chinese hamster) subset of the UniProtKB/Swiss-Prot database. The database search settings were specific for trypsin digestion. Specified modifications included dynamic Met oxidation and static Cys carbamidomethylation. Identifications were filtered to a strict protein false discovery rate (FDR) of 1% and relaxed FDR of 5% using the Percolator node in Proteome Discoverer.

2.5 | Relative quantification of individual HCPs and bound protein analysis

Relative quantity of each protein across samples was calculated based on the spectral count (SpC) for each protein (Cooper, Feng, & Garrett, 2010) in individual samples multiplied by the sample volume. The spectral abundance factor (SAF) of individual proteins in the collected supernatant samples (combination of the unbound fraction from the static binding and the following wash) was calculated as follows:

$$\mathrm{SAF}_{i,j} = \frac{SpC_{i,j} \times DF_j}{L_i},$$

wherein $\mathrm{SAF}_{i,j}$ is the spectral abundance factor for protein i in sample j (kDa^{-1}), SpC_i is the spectral count of protein i in sample j, DF_j is the dilution factor for sample j, and L_i is the molecular weight of protein i (kDa). The relative abundance of every HCP in the feed sample was calculated based on normalized spectral abundance factor (Neilson, Keighley, Pascovici, Cooke, & Haynes, 2013) for each identified protein calculated as follows:

$$\mathrm{NSAF}_i = \frac{\mathrm{SAF}_i}{\sum \mathrm{SAF}}.$$

A comparison of the relative quantities of individual HCPs in the supernatant versus feed samples was conducted by analysis of variance (ANOVA) of the SAF for every protein in the corresponding samples using JMP Pro 14. For the analysis of bound HCPs, the SAF values were used to compare the residual amounts of every HCP in the supernatants obtained by static binding of their corresponding feed samples. "Bound HCPs" are herein defined as the proteins that (a) were identified in the majority of feed samples (i.e., had a sum of spectral count greater than 4 across all replicates, $N = 3$) and (b) were either not found in the supernatant samples or showed statistically significantly (hereafter, "significantly") lower spectral count ($p < .05$ by ANOVA) compared to the feed sample. Venn diagrams of bound proteins across peptide-based and benchmark resins were constructed using the Venn Diagram add-in for JMP Pro 14. The non-normal distributions for isoelectric points of depleted proteins were compared by Kruskal–Wallis H test with a 90% confidence interval using JMP Pro 14.

3 | RESULTS AND DISCUSSION

3.1 | HCP distribution in load material

To determine the HCP composition in the CHO-K1 IgG-producing clarified harvest, proteomic analysis was performed on the feed material before diafiltration. The isoelectric point (pI), the grand average of hydropathy (GRAVY), and estimated protein abundance (data point diameter) were determined computationally based on the amino acid sequence of each protein identified by nano-LC-MS/MS. GRAVY is a metric for hydrophobicity determined as the sum of the contributions of each amino acid in the protein sequence based on the water-vapor transfer free energies and interior-exterior distribution of amino acid side chains (Kyte, Doolittle, Diego, & Jolla, 1982). Negative GRAVY value indicates hydrophilic character, whereas positive indicates hydrophobicity. Theoretical pI and MW were calculated using the ExPASy Bioinformatics Resource Portal

Compute pI/Mw tool (Swiss Institute of Bioinformatic), while GRAVY values were calculated using the GRAVY Calculator (Fuch). While sequence-based theoretical GRAVY and pI values do not rigorously represent the relative hydrophobicity and isoelectric point of large proteins, which are also determined by the tertiary and quaternary structures, this parameterization was used to offer a global picture of the HCP species diversity and gain a species-by-species-based understanding of important considerations for identifying ligands for HCP capture. Calculated molecular weights are represented by the color of the data point. This analysis resulted in the identification and relative quantification of 427 unique protein species, the majority of which were hydrophilic (GRAVY < 0), acidic (pI < 7), and had a molecular weight lower than 100 kDa. Figure 1 summarizes the properties and estimated abundance of each protein identified in the harvest.

It was desirable to quantitatively define the average properties of the global HCP population to better select the conditions for HCP capture. To this end, protein frequency was determined over the range of pI and GRAVY metrics. While not accounting for protein structure, the reported values of GRAVY are useful in evaluating the overall character of a protein population as a set of predominantly hydrophilic or hydrophobic species. The calculations returned negative GRAVY values for the large majority (92%) of the CHO-S HCPs. This result is reasonable, given that hydrophobic species are less likely to exist among proteins secreted by CHO-S cells in the aqueous extracellular space. Thus, clarification procedures without cell lysis result in harvest material that is likely to be rich in extracellular proteins with low abundance of membrane and intracellular components. With respect to the observed pI values, a typical bimodal isoelectric point distribution for eukaryotic organisms was observed, aligning with expected distribution despite the use of theoretical rather than empirical pI values, with a majority of proteins (74%) identified as acidic species (pI < 7), that is, negatively charged at neutral pH.

3.2 | Analysis of HCP binding

The CHO HCP-targeting peptide ligands discovered in prior work by screening tetrameric ($X_1X_2X_3X_4$GSG) and hexameric ($X_1X_2X_3X_4X_5X_6$GSG) peptide libraries comprise MP and HP peptides (Lavoie et al., 2019). MP ligands include sequences with one positively charged (Arg, His, Lys) and one negatively charged (Asp) amino acid residue, with the remaining combinatorial positions filled with aliphatic or aromatic residues. HP ligands include sequences containing one or two positively charged residue(s), with the remainder primarily aromatic residues. The initial characterization of these peptide-based adsorbents led to the identification of buffer conditions that maximize binding specificity for CHO HCPs over the IgG product. To that end, the peptide-based resins were compared to commercial resins Capto Q, a strong anion exchange resin featuring a quaternary amine ligand, and Capto Adhere, a mixed-mode resin featuring a combination of strong anion exchange, hydrogen bonding, and hydrophobic functionalities. The binding studies were conducted in static binding mode using a set of different binding buffers (NaCl concentration of 20 or 150 mM; pH 6, 7, or 8). The salt concentration and pH of buffers were selected to evaluate the performance of the resins at "harvest-like" conditions (150 mM NaCl) and "conventional polishing" conditions (20 mM NaCl). The pH range was limited to 6–8 to prevent protein instability in the clarified harvest. The feed samples were prepared by diafiltration of the cell culture fluid against the different buffers, incubated for 1 hr with the equilibrated adsorbents, and the supernatants (unbound and wash fraction) were collected and pooled before analysis. The resulting performance of each resin as a function of buffer condition by total HCP and IgG bound as reported in Lavoie et al. (2019) is summarized in Table 1.

The majority of the resins yielded the highest selectivity (where resin HCP selectivity was defined as the percent of HCP bound over the percent of IgG bound) at 20 mM NaCl, pH 7; based on global quantification of HCPs by enzyme-linked immunosorbent assay (ELISA), it was found that MP resins had equivalent or increased selectivity for HCPs compared to Capto Q and Capto Adhere

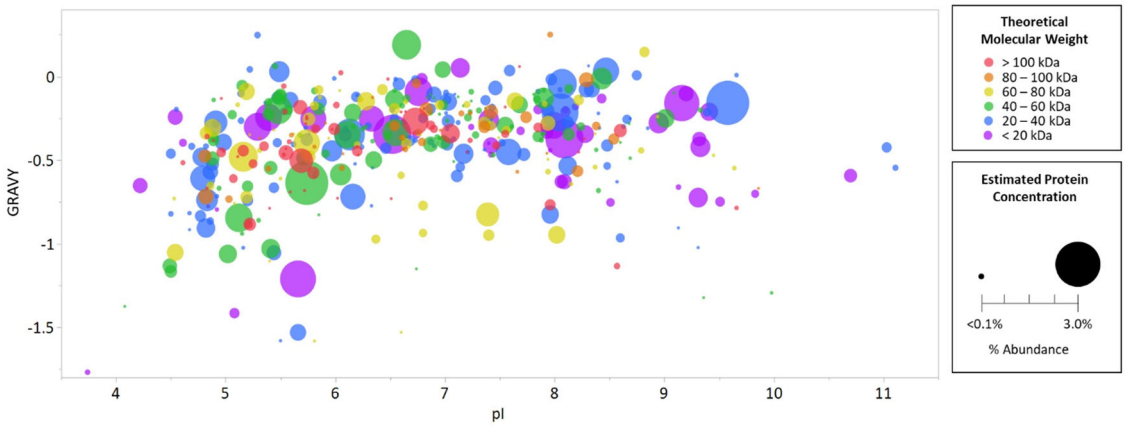

FIGURE 1 Bubble plot distribution of Chinese hamster ovary (CHO) host cell protein (HCP) species in monoclonal antibody (mAb) production harvest used as load material by theoretical molecular weight (MW), isoelectric point (pI), grand average of hydropathy (GRAVY), and calculated percent molar abundance. Each data point represents a unique protein identified in the harvest material. GRAVY values were determined using the GRAVY Calculator (Fuchs). All data further data with the exception of GRAVY values were obtained from Thermo Proteome Discoverer as described in Section 2.4 [Color figure can be viewed at wileyonlinelibrary.com]

TABLE 1 Percent bound monoclonal antibody and host cell protein in addition to resin selectivity by resin and buffer condition at 5 mg HCP/ml resin load

		20 mM NaCl			150 mM NaCl		
Resin	**Output**	**pH 6**	**pH 7**	**pH 8**	**pH 6**	**pH 7**	**pH 8**
6HP	Percent HCP bound	69.5 ± 4.8	79.3 ± 2.0	61.8 ± 5.1	86.4 ± 5.5	42.9 ± 5.0	9.4 ± 5.9
	Percent mAb bound	48.4 ± 4.4	48.7 ± 1.9	46.2 ± 0.5	48.9 ± 6.0	52.8 ± 5.5	61.8 ± 3.0
	Resin HCP selectivity	1.441 ± 0.114	1.630 ± 0.034	1.336 ± 0.098	1.783 ± 0.199	0.813 ± 0.030	0.151 ± 0.093
6MP	Percent HCP bound	71.9 ± 6.0	73.5 ± 6.5	59.4 ± 2.3	92.8 ± 3.8	53.9 ± 7.3	14.0 ± 8.8
	Percent mAb bound	51.0 ± 5.4	33.4 ± 11.9	40.0 ± 3.3	33.0 ± 10.0	50.9 ± 10.9	52.3 ± 7.5
	Resin HCP selectivity	1.428 ± 0.256	2.445 ± 1.083	1.488 ± 0.086	2.961 ± 0.742	1.109 ± 0.373	0.269 ± 0.166
4HP	Percent HCP bound	64.4 ± 11.1	75.4 ± 4.2	79.2 ± 1.8	87.0 ± 1.3	72.0 ± 2.3	48.6 ± 3.4
	Percent mAb bound	38.6 ± 9.4	46.6 ± 9.5	42.7 ± 1.0	47.4 ± 8.1	55.3 ± 4.3	62.0 ± 4.7
	Resin HCP selectivity	1.670 ± 0.298	1.620 ± 0.212	1.855 ± 0.032	1.836 ± 0.172	1.301 ± 0.084	0.784 ± 0.103
4MP	Percent HCP bound	58.0 ± 7.3	76.9 ± 5.1	76.9 ± 3.6	87.7 ± 5.1	67.8 ± 1.8	35.3 ± 8.4
	Percent mAb bound	31.1 ± 3.1	15.8 ± 4.1	23.5 ± 4.0	43.2 ± 7.8	55.9 ± 3.6	56.6 ± 3.0
	Resin HCP selectivity	1.863 ± 0.162	4.868 ± 0.266	3.279 ± 0.177	2.029 ± 0.190	1.214 ± 0.069	0.625 ± 0.244
Capto Adhere	Percent HCP bound	68.6 ± 13.0	70.3 ± 5.9	74.0 ± 4.0	77.1 ± 9.9	70.6 ± 1.5	33.1 ± 3.3
	Percent mAb bound	81.0 ± 3.0	94.7 ± 1.0	97.7 ± 2.2	72.3 ± 1.8	84.5 ± 1.5	93.1 ± 1.1
	Resin HCP selectivity	0.847 ± 0.193	0.743 ± 0.085	0.758 ± 0.058	1.067 ± 0.130	0.835 ± 0.028	0.355 ± 0.100
Capto Q	Percent HCP bound	62.7 ± 2.9	83.7 ± 3.4	76.0 ± 2.6	84.7 ± 6.8	61.1 ± 6.4	40.2 ± 7.5
	Percent mAb bound	37.7 ± 13.7	37.6 ± 11.7	64.8 ± 2.6	45.8 ± 8.9	48.1 ± 7.5	57.0 ± 2.9
	Resin HCP selectivity	1.664 ± 0.365	2.226 ± 0.313	1.174 ± 0.052	1.852 ± 0.210	1.270 ± 0.187	0.705 ± 0.193

Note. This table is adapted from Lavoie et al. (2019) Table B.1.

(Lavoie et al., 2019). HP resins, while slightly less selective than Capto Q, still exhibited preferential binding to HCPs and were found to be superior to Capto Adhere under the near-neutral pH conditions tested. The peptide-based resins also proved more effective than commercial resins in HCP binding studies performed at "harvest-like" condition (150 mM NaCl), suggesting potential use as pre-Protein A HCP scrubbers. These conditions were not specifically optimized for flow-through operation of commercial

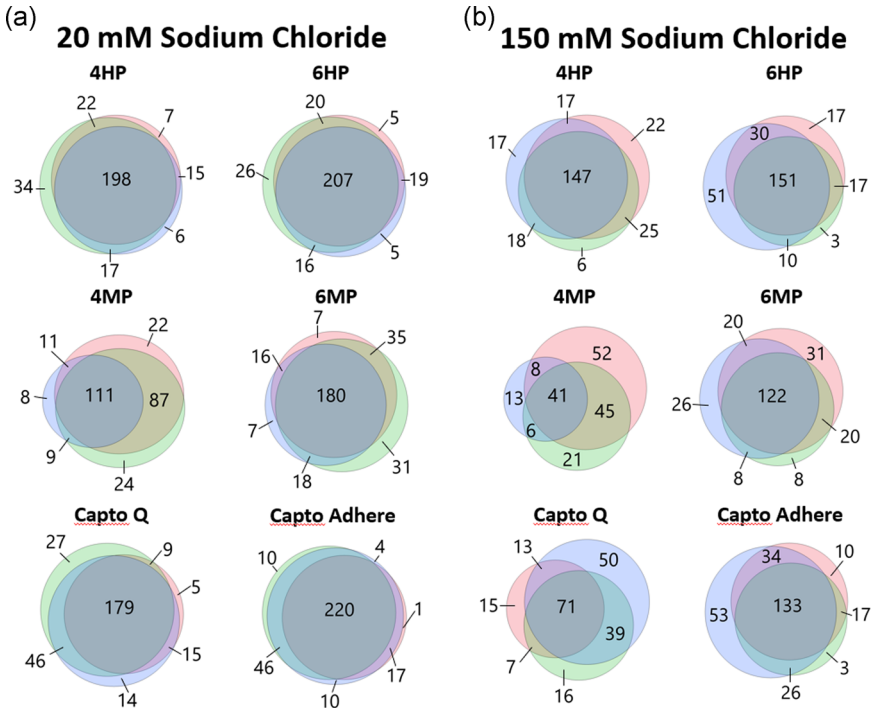

FIGURE 2 Overlapping HCPs bound at 20 mM NaCl and 150 mM NaCl by peptide-based resins (4HP, 6HP, 4MP, and 6MP) and benchmark resins (Capto Q and Capto Adhere) at pH 6 (pink), pH 7 (green), and pH 8 (blue). Bound proteins were determined as proteins that either were identified by liquid chromatography coupled to tandem mass spectrometry (LC–MS/MS) in the feed but not in the supernatant samples with wash after static binding with each resin, or alternatively where the resulting spectral abundance factor was significantly lower by analysis of variance (ANOVA; $\alpha = 0.05$) than the feed. The "overlap", or number of unique species of proteins that were bound at more than one pH condition for the range tested (pH 6, 7, and 8), is shown in the overlapping region of the Venn diagrams. HCP, host cell protein. [Color figure can be viewed at wileyonlinelibrary.com]

TABLE 2 Kruskal–Wallis *H* test for bound protein isoelectric point as a function of buffer pH using JMP Pro 14

		20 mM NaCl				150 mM NaCl			
Resin	pH	Mean rank score	Median pI	χ^2	*p*	Mean rank score	Median pI	χ^2	*p*
4HP	6	357.7	6.28	3.53	.171	300.0	6.25	2.07	.355
	7	393.3	6.62			293.0	6.2		
	8	371.7	6.47			317.5	6.52		
6HP	6	372.6	6.37	1.88	.392	302.0	6.16	9.51	.0086
	7	398.4	6.61			301.8	6.09		
	8	379.9	6.46			348.3	6.64		
4MP	6	292.8	6.33	0.839	.658	148.8	5.88	11.8	.0028
	7	305.8	6.54			164.1	6.23		
	8	306.6	6.52			196.4	6.82		
6MP	6	348.5	6.28	2.79	.248	257.4	6.16	3.89	.143
	7	378.5	6.62			251.8	6.12		
	8	356.8	6.43			282.2	6.53		
Capto Q	6	335.9	6.12	4.67	.0969	189.8	5.71	6.28	.0434
	7	375.4	6.54			197.9	5.74		
	8	369.7	6.54			223.4	6.13		
Capto Adhere	6	386.6	6.42	2.858	.240	290.2	6.18	8.69	.0130
	7	417.5	6.67			295.8	6.23		
	8	416.6	6.65			335.9	6.65		

Note. The distribution of isoelectric points for each unique bound protein were plotted by frequency of isoelectric point, but are not weighted based on abundance.
Abbreviation: pI, isoelectric point.

resins; Capto Q is in fact normally operated at low salt conditions, whereas Capto Adhere is utilized at fairly low pH values to prevent binding of the mAb product. The scope of this study, however, is to directly compare peptide-based and commercial resins under equivalent buffer conditions to highlight the ability of peptide ligands to capture HCPs efficiently and selectively without requiring extensive process optimization.

To further interrogate the observed differences in binding selectivity across the whole panel of resins, the present study focuses on the identification and relative quantification of individual HCPs. In this study, the HCPs in the supernatant samples from the static binding experiments were identified and quantified via bottom-up, label-free proteomics, and the resulting values were used to evaluate differences in binding of the various HCP groups by the peptide-based resins in

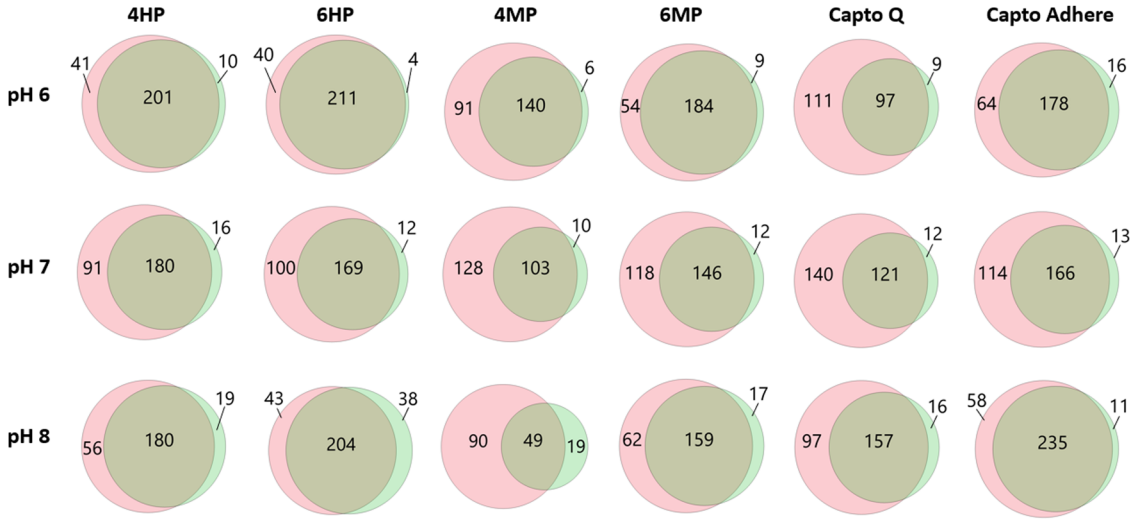

FIGURE 3 Overlapping HCPs bound at pH 6, 7, and 8 by peptide-based resins (4HP, 6HP, 4MP, and 6MP) and benchmark resins (Capto Q and Capto Adhere) at 20 mM (pink), 150 mM (green). Bound proteins were determined as proteins that either were identified by LC–MS/MS in the feed but not in the supernatant samples with wash after static binding with each resin, or alternatively where the resulting spectral abundance factor was significantly lower by ANOVA ($\alpha = 0.05$) than the feed. The "overlap", or number of unique species of proteins that were bound at both salt concentrations (20 and 150 mM) for the range tested (pH 6, 7, and 8), is shown in the overlapping region of the Venn diagrams. ANOVA, analysis of variance; HCP, host cell protein; LC–MS/MS, liquid chromatography coupled to tandem mass spectrometry [Color figure can be viewed at wileyonlinelibrary.com]

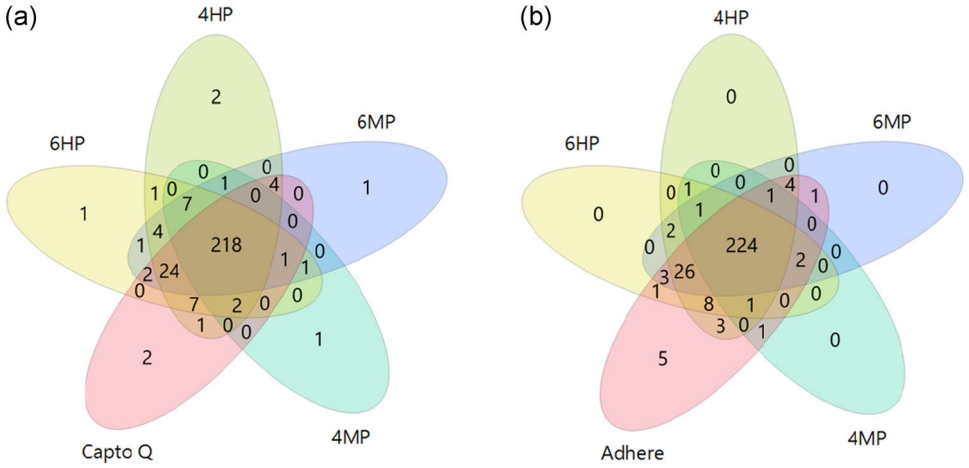

FIGURE 4 Overlapping bound proteins by peptide resins at pH 7, 20 mM NaCl. Bound proteins were determined as proteins that either were identified by LC–MS/MS in the feed but not in the supernatant samples with wash after static binding with each resin, or alternatively where the resulting dilution-adjusted spectral count was significantly lower by ANOVA ($\alpha = 0.05$) than the spectral count in the feed. Panel (a) compares the number of unique species bound to the novel peptide resins (4HP, 6HP, 4MP, and 6MP) to the Capto Q benchmark resin, and panel (b) compares the peptide resins to the Capto Adhere benchmark resin. ANOVA, analysis of variance; LC–MS/MS, liquid chromatography coupled to tandem mass spectrometry [Color figure can be viewed at wileyonlinelibrary.com]

comparison with the benchmark commercial resins. In this study, a "bound HCP" was defined as a protein that (a) is detected in the feed stream by LC/MS/MS analysis and (b) is either not detected in the supernatant (unbound+wash) or has a significantly lower SAF compared to the feed sample ($p < .05$ by ANOVA). SAF and ANOVA results are tabulated in Supporting Information section S.1 (Table S.1.A–F).

3.2.1 | Profile of bound HCPs versus ph of the binding buffer

The number of unique HCPs bound by the peptide-based and the commercial benchmark resins at different pH conditions are presented in Figure 2. The analysis of overlapping bound HCPs for the various resins as a function of buffer condition indicates that both 4HP and 6HP resins feature a higher tolerance to differences in pH compared to the benchmark and MP resins, at both salt concentrations (20 and 150 mM). As shown in Figure 2, of all unique bound HCPs across the three values of pH, 4HP, and 6HP, respectively, bound 66.2% (198 of 299 unique proteins) and 69.4% (207 of 298) at 20 mM NaCl, while 58.3% (147 of 199) and 54.1% (151 of 279) at 150 mM NaCl. In comparison, benchmark anion exchange resin Capto Q yielded 60.7% (179 of 295) at 20 mM and 33.6% (71 of 211) at 150 mM. Lower HCPs binding by Capto Q at a high salt concentration was anticipated, given that this resin relies

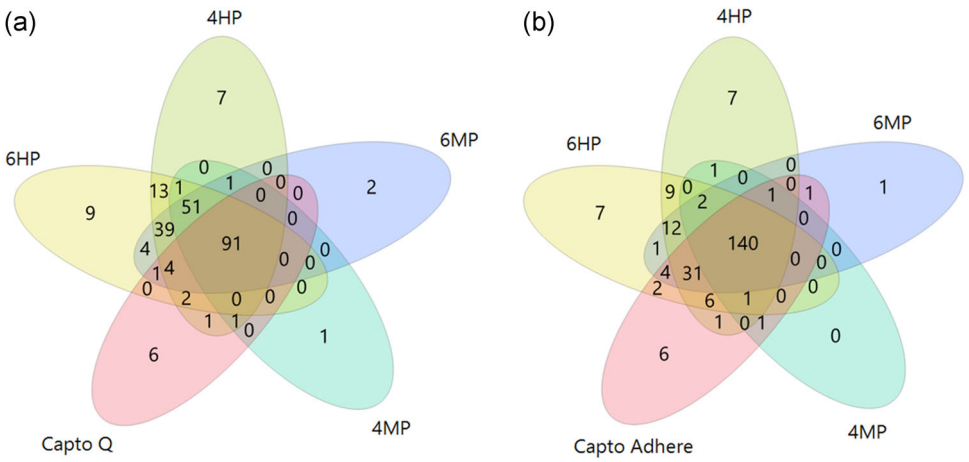

FIGURE 5 Overlapping bound proteins by peptide resins at pH 6, 150 mM NaCl. Bound proteins were determined as proteins that either were identified by LC–MS/MS in the feed but not in the supernatant samples with wash after static binding with each resin, or alternatively where the resulting dilution-adjusted spectral count was significantly lower by ANOVA ($\alpha = 0.05$) than the spectral count in the feed. Panel (a) compares the number of unique species bound to the novel peptide resins (4HP, 6HP, 4MP, and 6MP) to the Capto Q benchmark resin, and panel (b) compares the peptide resins to the Capto Adhere benchmark resin. ANOVA, analysis of variance; LC–MS/MS, liquid chromatography coupled to tandem mass spectrometry [Color figure can be viewed at wileyonlinelibrary.com]

TABLE 3 Problematic HCPs at pH 6, 150 mM by bound novel peptide resins that do not bind Capto Q

Problematic HCP group	HCP species
Group I (Protein A co-eluting)	Heat shock cognate protein Pyruvate kinase 60S acidic ribosomal protein P0 Elongation factor 2 Nidogen-1 Elongation factor 1-α Cofilin-1 Out-at-first protein-like protein Aldose reductase-related protein 2 Peroxiredoxin-1 Biglycan Glutathione s-transferase α-Enolase Glyceraldehyde-3-phosphate dehydrogenase Cathepsin B Matrix metalloproteinase-9 Matrix metalloproteinase-19 Protein disulfide-isomerase Serine protease HTRA1 Glutathione s-transferase
Group II (product degradation-associated)	Cathepsin B Matrix metalloproteinase-9 Matrix metalloproteinase-19 Protein disulfide-isomerase Serine protease HTRA1
Group III (highly immunogenic)	Glutathione s-transferase Phospholipase B-like protein Procollagen-lysine,2-oxoglutarate 5-dioxygenase 1 Peroxiredoxin-1

Abbreviation: HCP, host cell protein

solely on electrostatic binding; further, increased binding of the mAb product (isoelectric point ~ 7.6) by Capto Q at pH 8 (64.8% ± 2.6% at 20 mM and 57.0% ± 2.9% at 150 mM) also reduces the number of binding sites available for HCP capture as shown in Table 1 (Lavoie et al., 2019). The mixed-mode resin Capto Adhere showed high overlap in bound HCPs (71.4%, 220 of 308) at low salt concentration; however, promiscuous binding of HCPs was also accompanied by significant loss of mAb product (>80% for all pH conditions; Lavoie et al., 2019). The analysis of protein binding at 150 mM NaCl showed a decrease in overlap of bound HCPs to 48.2% (133 of 276 bound proteins), indicating poor tolerance to pH variations. The ability of HP resins to maintain HCP binding almost constant under different pH conditions suggests that the peptide ligands feature a stronger affinity-like binding activity than commercial mixed-mode ligands, which often require extensive optimization of process conditions to grant sufficient product yield and purity. Robustness in HCP capture within a design space of buffer conditions by peptide ligands makes them more apt towards platform processes for mAb purification.

Turning to MP ligands, 4MP and 6MP resins showed rather conspicuous differences in HCP binding. The 6MP resin compared well with its HP counterparts in terms of robustness of HCP capture against different pH conditions, with overlaps of bound HCPs of 61.2% (180 of 294) and 51.9% (122 of 235) at 20 mM and 150 mM, respectively. The 4MP ligand, on the other hand, demonstrated poor tolerance to pH differences at both 20 and 150 mM NaCl, with overlaps of bound HCPs of 40.8% (111 of 272) and 22.0% (41 of 186), respectively. A unique feature of the 4MP resin was its inverse relationship between HCP binding and buffer pH. As the net charge of the proteins in solution is shifted toward negative values as the pH of the binding buffer increases, the presence of negatively charged amino acids in the 4MP peptide ligands explains the loss of HCP binding at higher pH.

A comparison of the distributions of pI values among the HCPs bound at different pH conditions was also performed using the Kruskal–Wallis *H* test to evaluate the shift in the charge profile of the HCPs in the supernatant versus feed samples. The Kruskal–Wallis *H* test, as shown in Table 2, was adopted given the non-normal distribution of the pI values. If HCP binding by the peptide-based resin were dominated by electrostatic interactions, the pI profiles of bound HCPs would differ considerably among different pH conditions; in particular, the median pI would be expected to increase at higher binding pH, as HCPs with higher pI values would become negatively charged and be captured by the positively charged HP ligands. Notably, no significant shift in the isoelectric point profile of bound proteins was observed for the 4HP resin ($p = .171$ and $p = .355$ for 20 and 150 mM NaCl, respectively), whereas the 6HP resin showed a statistically significant shift only for the 150 mM NaCl condition ($p = .392$ and $p = .0086$ for 20 and 150 mM NaCl, respectively). This indicates that HCP–peptide interactions for 4HP and 6HP are not entirely dependent on electrostatic interaction; for comparison, the traditional anion exchange resin Capto Q shows a significant increase in pI as a function of pH at both salt conditions ($p = .0969$ at 20 mM and $p = .0434$ at 150 mM). Capto Adhere, whose ligand (whose 2-benzyl,2-hydroxyethyl,2methyl-ammonioethyl) has a strong similarity with the HP peptides, showed nonsignificant response in terms of pI distribution of bound HCPs versus pH at low salt and ($p = .240$ at 20 mM), but significant at high salt ($p = .0130$ at 150 mM). With multipolar ligands, a significant correlation between pH of binding and pI profile of bound HCPs was observed only with the 4MP resin at the high salt condition ($p = .0028$). The presence of both positive and negatively charged residues on MP ligands makes their interaction with HCPs more complex; the softening of electrostatic repulsions at high ionic strength allows the 4MP ligands to behave more similarly to conventional ion exchangers. Collectively, our results indicate a stronger correlation between binding pH and pI profile of bound HCPs at higher ionic strength of the binding buffer (150 mM vs. 20 NaCl, Table S.2.A). This result may be caused not only by a shift in HCP–peptide binding strength at different salt concentrations (Tsumoto, Ejima, Senczuk, Kita, & Arakawa, 2007), but also by a decrease in nonspecific adsorption of the highly abundant mAb product, which furthers the availability of binding sites for HCP capture.

3.2.2 | Profile of bound proteins versus ionic strength of the binding buffer

Overlap in bound HCPs as a function of ionic strength was additionally assessed to compare the tolerance of the different ligands to salt concentration. The comparison of HCP binding at

TABLE 4 Tabulated spectral abundance factor and ANOVA of CHO problematic HCPs by Capto Q, Capto Adhere, and HCP-binding peptide resins at pH 7, 20 mM sodium chloride

Protein	Uniprot Accession Number	Group I	Group II	Group III	Mean Spectral Abundance Factor						Capto Q Comparison ANOVA p-value				Capto Adhere Comparison ANOVA p-value			
					4HP	6HP	4MP	6MP	Capto Q	Capto Adhere	4HP	6HP	4MP	6MP	4HP	6HP	4MP	6MP
Biglycan	A0A061HUR7	X			<LOD	<LOD	<LOD	<LOD	0.0085 ± 0.015	<LOD	0.3739	0.3739	0.3739	0.3739	1	1	1	1
Heat shock cognate protein	A0A061I5D1	X			<LOD	<LOD	0.048 ± 0.0082	0.0093 ± 0.016	<LOD	<LOD	1	1	0.0006*	0.3739	1	1	0.0006*	0.3739
Fructose-bisphosphate aldolase	A0A061IB69	X			0.0081 ± 0.014	0.0084 ± 0.014	<LOD	0.015 ± 0.013	0.016 ± 0.014	<LOD	0.5314	0.5484	0.1163	0.9114	0.3739	0.3739	1	0.1196
Heat shock protein	A0A061ID29	X	X		<LOD	0.028 ± 0.049	0.027 ± 0.047	<LOD	<LOD	<LOD	1	0.3739	0.3739	1	1	0.3739	0.3739	1
Lipoprotein lipase	A0A061IKA1	X	X		<LOD	<LOD	<LOD	<LOD	<LOD	<LOD	1	1	1	1	1	1	1	1
Pyruvate kinase	A0A098KXC0	X			<LOD	<LOD	0.0086 ± 0.015	<LOD	<LOD	0.0086 ± 0.0075	1	1	0.3739	1	0.1163	0.1163	0.9973	0.1163
Sialidase I	B8Y440		X		<LOD	<LOD	<LOD	<LOD	<LOD	<LOD	1	1	1	1	1	1	1	1
Actin, cytoplasmic 1	G3GVD0	X			<LOD	<LOD	<LOD	0.017 ± 0.029	<LOD	0.017 ± 0.015	1	1	1	0.3739	0.1163	0.1163	0.1163	0.9873
Phosphoglycerate mutase 1	G3GZW8	X			<LOD	<LOD	<LOD	<LOD	<LOD	<LOD	1	1	1	1	1	1	1	1
Cathepsin B	G3H0L9	X	X		<LOD	0.010 ± 0.017	0.0093 ± 0.016	0.019 ± 0.016	0.098 ± 0.060	0.14 ± 0.054	0.0476*	0.0707	0.0692	0.0928	0.0112*	0.0167*	0.0163*	0.0210*
Peptidyl-prolyl cis-trans isomerase	G3H533	X			0.37 ± 0.085	0.40 ± 0.046	0.059 ± 0.023	0.17 ± 0.052	0.44 ± 0.094	0.16 ± 0.070	0.4219	0.6407	0.0025*	0.0130*	0.0321*	0.0076*	0.07	0.8867
Actin, alpha cardiac muscle 1	G3H5Q0	X			<LOD	<LOD	<LOD	<LOD	<LOD	<LOD	1	1	1	1	1	1	1	1
Matrix metalloproteinase-9	G3H8V1	X	X		<LOD	<LOD	<LOD	<LOD	<LOD	<LOD	1	1	1	1	1	1	1	1
Protein disulfide-isomerase A6	G3HB04	X	X		<LOD	<LOD	<LOD	<LOD	<LOD	<LOD	1	1	1	1	1	1	1	1
Vimentin	G3HHR3	X			<LOD	<LOD	<LOD	<LOD	<LOD	<LOD	1	1	1	1	1	1	1	1
Thrombospondin-1	G3HHV4	X			<LOD	<LOD	0.012 ± 0.020	<LOD	0.0059 ± 0.010	<LOD	0.3739	0.3739	0.6816	0.3739	1	1	0.3739	1
60S acidic ribosomal protein P0	G3HKG9	X			<LOD	<LOD	<LOD	<LOD	<LOD	<LOD	1	1	1	1	1	1	1	1
Clusterin	G3HNJ3	X			0.021 ± 0.00028	0.014 ± 0.024	0.10 ± 0.093	0.032 ± 0.030	0.092 ± 0.062	0.061 ± 0.021	0.1159	0.1095	0.9006	0.2003	0.0314*	0.0639	0.5109	0.2378
Matrix	G3HRK9	X	X		<LOD	<LOD	<LOD	<LOD	<LOD	<LOD	1	1	1	1	1	1	1	1

Protein	Uniprot Accession Number	Group I	Group II	Group III	Mean Spectral Abundance Factor						Capto Q Comparison ANOVA p-value				Capto Adhere Comparison ANOVA p-value			
					4HP	6HP	4MP	6MP	Capto Q	Capto Adhere	4HP	6HP	4MP	6MP	4HP	6HP	4MP	6MP
metalloproteinase-19																		
Elongation factor 2	G3HSL4	X			<LOD	<LOD	0.0036 ± 0.0063	0.0036 ± 0.0062	<LOD	0.0073 ± 0.0063	1	1	0.3739	0.3739	0.1163	0.1163	0.5163	0.5076
Nidogen-1	G3HWE4	X			<LOD	0.010 ± 0.017	0.0044 ± 0.0077	0.0044 ± 0.0076	<LOD	0.0091 ± 0.016	1	0.3739	0.3739	0.3739	0.3739	0.9712	0.669	0.6639
Legumain	G3I1H5		X		<LOD	<LOD	0.035 ± 0.061	<LOD	<LOD	<LOD	1	1	0.3739	1	1	1	0.3739	1
Glyceraldehyde-3-phosphate dehydrogenase	G3I1S5	X			<LOD	<LOD	<LOD	<LOD	<LOD	<LOD	1	1	1	1	1	1	1	1
Sulfated glycoprotein 1	G3I1Y9	X			<LOD	<LOD	0.24 ± 0.055	0.024 ± 0.021	0.11 ± 0.079	0.10 ± 0.060	0.0815	0.0815	0.0689	0.1564	0.0415*	0.0415*	0.0407*	0.0968
Glutathione S-transferase P	G3I3Y6	X		X	<LOD	<LOD	<LOD	0.014 ± 0.024	<LOD	<LOD	1	1	1	0.3739	1	1	1	0.3739
Cathepsin D	G3I4W7	X	X		<LOD	<LOD	0.055 ± 0.036	0.022 ± 0.021	<LOD	<LOD	1	1	0.056	0.1399	1	1	0.056	0.1399
Phospholipase B-like protein	G3I6T1			X	<LOD	<LOD	0.0051 ± 0.0089	<LOD	<LOD	<LOD	1	1	0.3739	1	1	1	0.3739	1
Endoplasmic reticulum BiP	G3I8R9		X		<LOD	<LOD	<LOD	<LOD	<LOD	<LOD	1	1	1	1	1	1	1	1
Alpha-enolase	G3IAQ0	X			0.023 ± 0.00031	0.0081 ± 0.014	0.075 ± 0.010	0.037 ± 0.015	0.015 ± 0.026	0.015 ± 0.013	0.618	0.7033	0.0209*	0.2846	0.3337	0.565	0.0032*	0.1333
Serine protease HTRA1	G3IBF4	X	X		0.013 ± 0.022	<LOD	0.013 ± 0.022	0.022 ± 0.020	0.038 ± 0.0014	0.037 ± 0.0008	0.1179	<.0001*	0.1197	0.2334	0.1374	<.0001*	0.1395	0.2791
Metalloproteinase inhibitor 1	G3IBH0	X			0.23 ± 0.030	0.28 ± 0.080	0.33 ± 0.054	0.23 ± 0.021	0.28 ± 0.11	0.14 ± 0.0030	0.4688	0.9954	0.5224	0.4459	0.0078*	0.0395*	0.0037*	0.0025*
Cofilin-1	G3IDM2	X			0.098 ± 0.034	0.080 ± 0.069	0.46 ± 0.12	0.12 ± 0.11	0.24 ± 0.16	0.094 ± 0.031	0.2033	0.1831	0.1238	0.3422	0.8924	0.7579	0.0073*	0.6978
Out at first protein-like	G3IEB7	X			<LOD	<LOD	<LOD	<LOD	<LOD	<LOD	1	1	1	1	1	1	1	1
Procollagen-lysine,2-oxoglutarate 5-dioxygenase 1	G3IIE7			X	<LOD	<LOD	<LOD	<LOD	<LOD	<LOD	1	1	1	1	1	1	1	1
Aldose reductase-related protein 2	O08782	X			<LOD	<LOD	<LOD	<LOD	<LOD	<LOD	1	1	1	1	1	1	1	1
Elongation factor 1-alpha	Q540F6	X			<LOD	<LOD	<LOD	<LOD	<LOD	<LOD	1	1	1	1	1	0.7522	1	1
Peroxiredoxin-1	Q9JKY1	X		X	0.016 ± 0.028	0.016 ± 0.028	0.14 ± 0.17	0.043 ± 0.041	0.26 ± 0.11	<LOD	0.0227*	0.0226*	0.3746	0.0355*	0.3739	0.3739	0.2165	0.1444

Note. Mean and standard deviation of spectral abundance factor (n = 3) are reported for each species. Calculated p-values for ANOVA comparisons of each peptide resin compared to both benchmark resins (Capto Q and Capto Adhere) are provided. Species identified by shotgun proteomics in this study identified as "problematic" based on prior art (Aboulaich et al., 2014; Bailey-Kellogg et al., 2014; Chiu et al., 2017; Fischer et al., 2017; Gagnon et al., 2014; Goey et al., 2018; Jawa et al., 2016; Levy et al., 2014; Mechetner et al., 2011; Zhang et al., 2016). *$p < .05$.

Abbreviations: ANOVA, analysis of variance; CHO, Chinese hamster ovary; HCP, host cell protein

20 mM versus 150 mM NaCl concentration is reported in Figure 3 for all resins and binding pH. Notably, the proteomic analysis of the supernatant samples obtained with peptide-based resins showed a strong tolerance to 150 mM, a typical salt concentration in clarified cell culture harvests. When tested at 150 mM NaCl, in fact, 4HP and 6HP ligands, in particular, maintained the binding of a significant fraction of HCPs (60.1–82.7%) demonstrated at 20 mM NaCl. As anticipated for an ion exchange resin, Capto Q showed a significant reduction in the number of HCPs bound as the salt concentration increased, and consequently a decrease in the number of overlapping bound proteins. Percent overlapping of bound HCPs by Capto Adhere was closer to the values obtained with HP resins (69.0–77.3%), but was also associated with considerably higher binding of the mAb product (~45–50% mAb bound for HP resins compared to ~95% for Capto Adhere), as previously reported (Lavoie et al., 2019) and summarized in Table 1. Multipolar resins 4MP and 6MP showed substantially different binding behavior as a function of salt concentration. Good salt tolerance, comparable to that of HP resins, was observed with 6MP resin, which provided an overlap in bound HCPs of 52.9–66.8%. On the contrary, 4MP resin showed low tolerance to salt concentration, similarly to what observed in response to pH conditions, corroborating the hypothesis that the binding activity of this family of ligands has a predominantly electrostatic character.

3.2.3 | Profile of bound proteins by peptide-based resins versus commercial resins

A comparison of the HCP species bound by the various resins at given binding conditions (pH and salt concentration) was then performed to identify proteins uniquely bound by a single or a set of resins. Our analysis focused on the optimal binding conditions identified in prior work (Lavoie et al., 2019), namely pH 7 at 20 mM NaCl and pH 6 at 150 mM NaCl, whose results of overlap of protein binding by the various resins are presented as Venn diagrams in Figure 4 and Figure 5. Analogous plots for the other binding conditions are available in Supporting Information section S.3 and Figure S.3.A–D.

Proteomic analysis of the fractions generated at 20 mM NaCl, pH 7 indicates substantial overlap in unique proteins bound between the peptide resins and the benchmark resins. Capto Q, in particular, afforded significant binding of 261 unique proteins, of which only two were not bound by any of the peptide resins, namely EF-HAND 2 containing protein and fatty acid-binding protein (adipocyte), neither of which has been reported as a problematic HCP to our knowledge. On the other hand, peptide resins showed significant binding of additional 20 unique HCP species, including problematic HCPs from Group I (peptidyl-prolyl *cis-trans* isomerase, fructose-bisphosphate aldolase, sulfated glycoprotein 1, glyceraldehyde 3-phosphate dehydrogenase, and biglycan). From the perspective of overall product purity, Group I Protein A co-eluting HCPs are the most challenging to address, as a large majority of these proteins are indicated to co-elute as a result of association to the product (Aboulaich et al., 2014; Levy et al., 2014) or association to histones that can in turn nonspecifically bind to multiple entities (Mechetner et al., 2011). The efficient capture of product-bound species in this group may explain to some degree the loss of IgG observed in prior work (Lavoie et al., 2019), as some IgG molecules may associate with the HCPs retained by the HP ligand. The HCP retention by the 6HP peptides matched the performance of Capto Adhere, a commercial mixed-mode ligand that possesses a broad and strong HCP binding capacity under these buffer conditions. 6HP showed significant binding of 15 of the 20 additional species, but failed to bind fructose-bisphosphate aldolase, which was captured only by 4MP, in addition to one form of peptidyl-prolyl cis-trans isomerase. It was further noted that in addition to the nearly 80% HCP bound by 4MP by HCP ELISA and high number of unique proteins bound, the 4MP ligand had the lowest observed percent mAb bound from the entire study at 15.8% ± 4.1% as shown in Table 1 (Lavoie et al., 2019).

In comparison to the benchmark mixed-mode resin, the peptide resins bound 280 of the 285 unique species bound by Capto Adhere, while also showing a considerably lower binding (>2-fold) of the mAb product (Lavoie et al., 2019), as shown in Table 1. Four HCP species, including problematic HCP sulfated glycoprotein 1, in addition to tenascin-X, copper transport protein ATOX1, and procollagen C-endopeptidase enhancer 1, were captured by one or more peptide-based resins, but did not show binding to Capto Adhere under these conditions. A large majority of the species bound by Capto Adhere (270 of 285) was also captured by the 6HP resin; this was expected, given similarities in the potential binding interactions between the two resins, despite significant differences in mAb product binding shown in Table 1.

A parallel analysis of the fractions generated at 150 mM NaCl, pH 6, summarized in Figure 5, indicates considerable differences in the capture of HCPs by the peptide resins versus the benchmark resins. As shown in Figure 5a, the peptide resins bound 128 unique proteins in addition to 100 of the 106 proteins bound by Capto Q, including problematic HCPs from all three problematic HCP groups. Problematic species bound by peptide resins, but not Capto Q are summarized in Table 3. A large majority (117 of 128) of the species that do not bind to Capto Q, but do bind to at least one peptide resin, showed binding to the 6HP resin. Notable exceptions include peptidyl-prolyl cis-trans isomerase, which was bound by 4HP and both MP resins, as well as biglycan, glutathione s-transferase P, α-enolase, and glyceraldehyde-3-phosphate dehydrogenase, which were only bound by 4HP. In comparison, of the 6 HCPs bound exclusively by Capto Q, only one has been reported as a problematic, namely 60S acidic ribosomal protein P2. The overlap of bound HCPs shown in Figure 5b indicates a broader binding by Capto Adhere compared to Capto Q, as well as a larger group of shared bound proteins between the peptide resins and Capto Adhere. Nonetheless, the peptide resins bound 40 more unique species than Capto Adhere while showing considerably lower mAb product binding as shown in Table 1.

TABLE 5 Tabulated spectral abundance factor and ANOVA of CHO problematic HCPs by Capto Q, Capto Adhere, and HCP-binding peptide resins at pH 6, 150 mM sodium chloride

Protein	Uniprot Accession Number	Group I	Group II	Group III	Mean Spectral Abundance Factor						Capto Q Comparison ANOVA p-value				Capto Adhere Comparison ANOVA p-value			
					4HP	6HP	4MP	6MP	Capto Q	Capto Adhere	4HP	6HP	4MP	6MP	4HP	6HP	4MP	6MP
Biglycan	A0A061HUR7	X			<LOD	0.018 ± 0.016	0.018 ± 0.015	0.018 ± 0.016	0.017 ± 0.029	0.019 ± 0.016	0.374	0.9463	0.9721	0.9623	0.1163	0.9781	0.9387	0.9538
Heat shock cognate protein	A0A061I5D1	X			0.074 ± 0.024	0.047 ± 0.015	0.38 ± 0.080	0.11 ± 0.027	0.49 ± 0.066	0.12 ± 0.022	0.0005*	0.0003*	0.1366	0.0008*	0.0697	0.0092*	0.0058*	0.7251
Fructose-bisphosphate aldolase	A0A061IB69	X			0.057 ± 0.012	0.060 ± 0.016	0.074 ± 0.026	0.066 ± 0.036	0.065 ± 0.015	0.060 ± 0.017	0.5008	0.7037	0.6246	0.9747	0.8078	1	0.467	0.8087
Heat shock protein	A0A061ID29	X	X		0.14 ± 0.050	0.15 ± 0.050	0.23 ± 0.047	0.11 ± 0.13	0.26 ± 0.088	0.12 ± 0.10	0.1197	0.1362	0.6596	0.1819	0.7513	0.6868	0.1699	0.9484
Lipoprotein lipase	A0A061IKA1	X	X		0.054 ± 0.030	0.014 ± 0.012	0.089 ± 0.025	0.075 ± 0.039	0.094 ± 0.013	0.036 ± 0.026	0.0993	0.0015*	0.7506	0.4613	0.4773	0.2581	0.0625	0.2235
Pyruvate kinase	A0A098KXC0	X			0.036 ± 0.015	0.028 ± 0.014	0.073 ± 0.0077	0.060 ± 0.029	0.13 ± 0.035	0.10 ± 0.031	0.0115*	0.0087*	0.0457*	0.0517	0.0332*	0.0230*	0.2254	0.183
Sialidase I	B8Y440		X		<LOD	<LOD	<LOD	<LOD	0.12 ± 0.016	<LOD	0.0002*	0.0002*	0.0002*	0.0002*	1	1	1	1
Actin, cytoplasmic 1	G3GVD0	X			<LOD	<LOD	0.17 ± 0.15	<LOD	0.37 ± 0.079	0.14 ± 0.14	0.0012*	0.0012*	0.1049	0.0012*	0.1632	0.1632	0.823	0.1632
Phosphoglycerate mutase 1	G3GZW8	X			<LOD	<LOD	0.13 ± 0.12	<LOD	0.220 ± 0.065	0.059 ± 0.10	0.0042*	0.0042*	0.3049	0.0042*	0.3739	0.3739	0.4766	0.3739
Cathepsin B	G3H0L9	X	X		0.039 ± 0.034	0.051 ± 0.034	0.32 ± 0.019	0.090 ± 0.0037	0.99 ± 0.059	0.092 ± 0.031	<.0001*	<.0001*	<.0001*	<.0001*	0.1151	0.1934	0.0004*	0.9137
Peptidyl-prolyl cis-trans isomerase	G3H533	X			1.3 ± 0.20	1.5 ± 0.062	1.30 ± 0.085	1.5 ± 0.43	1.30 ± 0.24	1.0 ± 0.28	0.8166	0.1933	0.9509	0.6013	0.1779	0.0378*	0.1589	0.2079
Actin, alpha cardiac muscle 1	G3H5Q0	X			<LOD	<LOD	<LOD	<LOD	<LOD	<LOD	1	1	1	1	1	1	1	1
Matrix metalloproteinase-9	G3H8V1	X	X		<LOD	<LOD	0.019 ± 0.022	<LOD	0.028 ± 0.013	<LOD	0.0234*	0.0234*	0.5983	0.0234*	1	1	0.2081	1
Protein disulfide-isomerase A6	G3HB04	X	X		<LOD	<LOD	0.026 ± 0.023	<LOD	0.053 ± 0.046	<LOD	0.1165	0.1165	0.4227	0.1165	1	1	0.1162	1
Vimentin	G3HHR3	X			<LOD	<LOD	0.028 ± 0.031	0.021 ± 0.020	0.11 ± 0.025	0.028 ± 0.012	0.0017*	0.0017*	0.0246*	0.0087*	0.0134*	0.0134*	0.9709	0.584
Thrombospondin-1	G3HHV4	X			0.043 ± 0.021	0.058 ± 0.038	0.037 ± 0.018	0.037 ± 0.017	0.024 ± 0.010	0.020 ± 0.020	0.2465	0.2227	0.3539	0.3327	0.2383	0.2038	0.3261	0.3122
60S acidic ribosomal protein P0	G3HKG9	X			<LOD	<LOD	<LOD	<LOD	0.012 ± 0.021	<LOD	0.3739	0.3739	0.3739	0.3739	1	1	1	1
Clusterin	G3HNJ3	X			0.092 ± 0.046	0.089 ± 0.0020	0.37 ± 0.049	0.17 ± 0.050	0.73 ± 0.15	0.28 ± 0.074	0.0021*	0.0018*	0.0169*	0.0035*	0.0189*	0.0105*	0.1544	0.0845
Matrix metalloproteinase-19	G3HRK9	X	X		<LOD	<LOD	0.019 ± 0.019	<LOD	0.025 ± 0.012	<LOD	0.0227*	0.0227*	0.6687	0.0227*	1	1	0.161	1
Elongation factor 2	G3HSL4	X			0.0039 ± 0.0068	0.0080 ± 0.0069	0.019 ± 0.018	0.012 ± 0.012	0.095 ± 0.018	0.016 ± 0.014	0.0012*	0.0015*	0.0065*	0.0026*	0.2445	0.4161	0.8165	0.6962
Nidogen-1	G3HWE4	X			0.0045 ± 0.0078	0.010 ± 0.0085	0.0093 ± 0.0081	0.0045 ± 0.0079	0.14 ± 0.0052	0.010 ± 0.0085	<.0001*	<.0001*	<.0001*	<.0001*	0.4737	0.991	0.946	0.4758
Legumain	G3I1H5		X		0.66 ± 0.060	0.90 ± 0.18	0.73 ± 0.15	0.58 ± 0.070	0.73 ± 0.059	0.67 ± 0.078	0.2518	0.1904	0.9327	0.053	0.9014	0.1133	0.5393	0.2295
Glyceraldehyde-3-phosphate dehydrogenase	G3I1S5	X			<LOD	<LOD	<LOD	<LOD	0.051 ± 0.089	<LOD	0.3739	0.3739	0.3739	0.3739	1	1	1	1
Sulfated glycoprotein 1	G3I1Y9	X			0.20 ± 0.043	0.30 ± 0.11	0.69 ± 0.069	0.41 ± 0.047	1.0 ± 0.054	0.45 ± 0.10	<.0001*	0.0005*	0.0030*	0.0001*	0.0179*	0.1518	0.0274*	0.5946
Glutathione S-transferase P	G3I3Y6	X		X	<LOD	0.031 ± 0.027	0.074 ± 0.026	0.029 ± 0.050	0.074 ± 0.026	0.030 ± 0.026	0.0083*	0.1234	0.9723	0.239	0.1161	0.9666	0.1072	0.9643
Cathepsin D	G3I4W7	X	X		0.25 ± 0.064	0.27 ± 0.026	0.28 ± 0.024	0.23 ± 0.063	0.22 ± 0.028	0.21 ± 0.052	0.4527	0.0695	0.0441*	0.7554	0.4552	0.1491	0.1122	0.7057
Phospholipase B-like protein	G3I6T1			X	0.0056 ± 0.010	<LOD	0.10 ± 0.016	0.029 ± 0.010	0.28 ± 0.093	0.018 ± 0.00055	0.0068*	0.0062*	0.0295*	0.0092*	0.101	<.0001*	0.0009*	0.1194
Endoplasmic reticulum BiP	G3I8R9		X		<LOD	0.011 ± 0.019	0.098 ± 0.025	<LOD	0.17 ± 0.030	<LOD	0.0006*	0.0014*	0.0302*	0.0006*	1	0.3739	0.0026*	1
Alpha-enolase	G3IAQ0	X			0.079 ± 0.038	0.17 ± 0.021	0.29 ± 0.053	0.17 ± 0.018	0.28 ± 0.098	0.22 ± 0.12	0.0275*	0.125	0.8895	0.1135	0.1086	0.4912	0.3966	0.4572
Serine protease HTRA1	G3IBF4	X	X		0.026 ± 0.023	0.040 ± 0.0009	0.039 ± 0.00076	0.038 ± 0.038	0.19 ± 0.036	0.12 ± 0.044	0.0025*	0.0019*	0.0018*	0.0069*	0.0282*	0.0324*	0.0306*	0.0671
Metalloproteinase inhibitor 1	G3IBH0	X			0.80 ± 0.048	0.91 ± 0.11	0.83 ± 0.25	0.84 ± 0.20	0.84 ± 0.11	0.72 ± 0.060	0.6755	0.4588	0.9611	0.9899	0.1325	0.0549	0.5022	0.3958
Cofilin-1	G3IDM2	X			0.62 ± 0.13	0.48 ± 0.086	1.2 ± 0.24	0.59 ± 0.19	1.7 ± 0.19	0.88 ± 0.14	0.0012*	0.0005*	0.0517	0.0021*	0.0754	0.0129*	0.0926	0.1023
Out at first protein-like	G3IEB7	X			<LOD	<LOD	0.086 ± 0.15	<LOD	0.11 ± 0.19	<LOD	0.3739	0.3739	0.8756	0.3739	1	1	0.3739	1
Procollagen-lysine,2-oxoglutarate 5-dioxygenase 1	G3IIE7			X	<LOD	<LOD	<LOD	<LOD	0.049 ± 0.011	1.0 ± 1.0	0.0014*	0.0014*	0.0014*	0.0014*	**1**	**1**	**1**	**1**
Aldose reductase-related protein 2	O08782	X			<LOD	0.011 ± 0.018	0.061 ± 0.030	<LOD	0.08 ± 0.032	0.011 ± 0.019	0.0119*	0.0304*	0.4879	0.0119*	0.3739	0.9842	0.0694	0.3739
Elongation factor 1-alpha	Q540F6	X			0.053 ± 0.091	<LOD	<LOD	<LOD	0.24 ± 0.043	0.064 ± 0.11	0.0352*	0.0007*	0.0007*	0.0007*	0.9015	0.3739	0.3739	0.3739
Peroxiredoxin-1	Q9JKY1	X		X	0.99 ± 0.182	0.92 ± 0.16	0.95 ± 0.26	0.98 ± 0.057	1.1 ± 0.14	0.89 ± 0.26	0.4817	0.0098*	0.5542	0.0210*	0.5982	0.8649	0.1423	0.5654

Note. Mean and standard deviation of spectral abundance factor ($n = 3$) are reported for each species. Calculated p-values for ANOVA comparisons of each peptide resin compared to both benchmark resins (Capto Q and Capto Adhere) are provided. Species identified by shotgun proteomics in this study identified as "problematic" based on prior art (Aboulaich et al., 2014; Bailey-Kellogg et al., 2014; Chiu et al., 2017; Fischer et al., 2017; Gagnon et al., 2014; Goey et al., 2018; Jawa et al., 2016; Levy et al., 2014; Mechetner et al., 2011; Zhang et al., 2016). *$p < .05$.

Abbreviations: ANOVA, analysis of variance; CHO, Chinese hamster ovary; HCP, host cell protein

3.3 | Semiquantitative evaluation of the binding of "problematic" HCPs by peptide resins versus benchmark resins

To gather a quantitative measure of the differences in HCP-binding activities of the peptide-based resins, label-free relative quantification based on proteomics analysis of the collected fractions was conducted by LC/MS/MS. Specifically, DDA methods were adopted to compare the relative SAF of every HCPs species in the supernatant samples obtained from static binding tests using the peptide-based resins and benchmark resins Capto Q and Capto Adhere.

This study was limited to the supernatant samples obtained at the conditions that proved most effective for HCP binding, namely 20 mM NaCl at pH 7, and 150 mM NaCl at pH 6 (Lavoie et al., 2019). The resulting values of SAF for problematic HCP species identified in the supernatants produced at 20 mM NaCl at pH 7 are listed in Table 4. These values of SAF were compared by an ANOVA ($n = 3$) between the peptide-based resins and both benchmark resins to evaluate the advantage of using peptide ligands for HCP removal. Significantly higher binding was observed for several problematic HCP species by the peptide-based resins compared to Capto Q: cathepsin B, serine protease HTRA1, peptidyl-prolyl cis-trans isomerase, peroxiredoxin-1. 6HP resin was particularly effective compared to Capto Q in binding Group I/II HCP serine protease HTRA1 and Group I/III HCP peroxiredoxin-1, and outperformed Capto Adhere, its small molecule cognate, in binding serine protease HTRA1. 4HP showed improved binding of Group I/II HCP cathepsin B compared to both Capto Adhere and Capto Q. Notably, the binding of peptidyl-prolyl cis-trans isomerase by both MP resins was significantly higher compared to Capto Q and on par with Capto Adhere; it should be noted, however, that the capture of this hard-to-clear species by Capto Adhere comes with a much higher cost in terms of mAb loss compared to MP resins, as summarized in Table 1. It was also observed that fructose-bisphosphate aldolase was depleted to levels below the limit of detection by 4MP alone amongst the peptide resins, although the difference in mean spectral counts was not statistically significant, matched only by the higher mAb product binding Capto Adhere.

The development of salt-tolerant stationary phases for mAb purification is much sought after, as they provide flexibility in process implementation. As a result, the binding of HCP species in 150 mM NaCl at pH 6, was analyzed. The values of total HCP clearance and HCP versus IgG binding determined by ELISA tests indicated that, at this condition, all four peptide-based resins performed equivalently or better than Capto Q (Lavoie et al., 2019).

Calculated SAF for HCP species at 150 mM NaCl by both peptide-based and benchmark resins are reported in Table 5. While increasing salt concentration resulted in an overall reduction in HCP binding, a marked improvement in capture by the peptide ligands was also observed compared to Capto Q. The HP resins were the most versatile in HCP capture, showing significantly higher binding for a large majority of the species in this subset compared to other resins. In particular, 4HP showed significantly lower spectral abundance (higher binding) for 21 of the 37 problematic HCPs, including 19 Group I HCPs and 6 Group II HCPs, 2 Group III HCPs (note that some HCPs are described by more than one group) compared to Capto Q. Furthermore, five of the 37 species tracked were more effectively bound to 4HP compared to Capto Adhere (pyruvate kinase, vimentin, clusterin, sulfated glycoprotein 1, and serine protease HTRA1). The remaining species in both cases showed no significant difference in spectral abundance, and, as a result, no problematic HCPs were found to be captured more effectively by Capto Q than 4HP. The 6HP resin was also successful in binding these HCPs compared to Capto Q, showing significantly lower spectral abundance for 22 of the 37 investigated species, including 19 Group I HCPs, 8 Group II, and 3 Group III HCPs. In comparison to Capto Adhere, seven of the 37 species were bound more effectively by 6HP. Only 1 HCP, Group I HCP peptidyl-prolyl cis-trans isomerase, showed statistically higher binding to Capto Adhere. Species more effectively captured by 4HP and 6HP compared to benchmark resins showed good agreement, as expected given similarities in peptide functional groups.

Among the peptide-based resins, 4MP showed the lowest improvement in HCP binding compared to Capto Q and Capto Adhere; nonetheless, improved problematic HCP capture was observed, and was noted to be associated with lower mAb product binding compared to Capto Adhere as shown in Table 1 and described in detail in prior work (Lavoie et al., 2019). Thirteen of the 37 considered species showed significantly lower spectral abundance (higher binding) compared to Capto Q, including nine Group I HCPs, four Group II HCPs, and two Group III HCPs. One HCP, Group I/II HCP Cathepsin D, was bound more effectively by Capto Q than 4MP, but overall, improved binding performance was observed. Capto Adhere binding of problematic HCPs outperformed 4MP only for five species, namely heat shock cognate protein, cathepsin B, sulfated glycoprotein 1, phospholipase B-like protein, and endoplasmic reticulum BiP; however, the high mAb product binding observed with this resin (see Table 1) would reduce the likelihood of its implementation. 4MP outperformed Capto Adhere with a single protein, Group I/II HCP serine protease HTRA1. While 4MP resin returned the lowest HCP binding performance, it should be noted that by both quantitative and qualitative measures, it outperforms quaternary amine ligands (Capto Q), which are currently employed on depth filtration media for clearing HCPs in harvest fluids that feature comparable salt concentration to that considered here (Gilgunn et al., 2019; Singh et al., 2017).

Finally, 6MP behaved similarly to 6HP in improving the clearance of HPC species compared to Capto Q, with the only exceptions of pyruvate kinase and lipoprotein lipase. Compared to Capto Adhere, no statistically significant difference was observed in the binding of the 37 species of problematic HCPs; however, a considerably lower binding of the mAb product was reported, confirming previous findings of enhanced selectivity compared to Capto Adhere (Lavoie et al., 2019).

4 | CONCLUSIONS

After identifying lead peptide ligand candidates for selective overall CHO HCP capture (Lavoie et al., 2019), qualitative evaluation of total number of HCPs bound by each resin was performed, and

problematic HCP species were identified that were more effectively bound by these novel ligands based on semiquantitative comparison of spectral abundance in static binding supernatants. The capture of these HCPs coupled with improved specificity for HCP over product IgG indicate that incorporation of these ligands in stationary phases for mAb purification could improve HCP clearance and robustness in mAb purification processes. The ability of these ligands to bind low percentages of IgG indicate that they are good candidates for weak partitioning mode chromatography to achieve the high HCP clearance needed for biotherapeutics. In addition, when used for capture in high salt conditions, the peptide resins, particularly hydrophobic positive resins, were observed to be more tolerant of physiological salt conditions, as tested at 150 mM NaCl. Improved binding of lipoprotein lipase, cathepsin B, matrix metalloproteinase-9, matrix metalloproteinase-19, endoplasmic reticulum BiP, serine protease HTRA1 and sialidase-1 at high salt were particularly promising, as this shows evidence that use of these ligands early in the purification process may help to limit product degradation by proteolytic cleavage. In addition, the maintained HCP capture despite increase salt concentration expands the possibilities for these ligands above and beyond what is possible with traditional anion exchange ligands by allowing for HCP "scrubbing" before product capture either by traditional FT chromatography immediately post-clarification, or by modification of depth filters with these ligands to enable enhanced capture of HCPs during clarification. Further work will focus on characterizing species removal when operated in flow-through or weak partitioning mode in dynamic binding applications to determine achievable HCP log reduction values possible with these novel stationary phases.

ACKNOWLEDGMENTS

The authors wish to thank Fujifilm Diosynth for their generous support and providing of IgG-producing cell culture harvest. They also wish to thank Kevin Blackburn from Waters Corporation and Michael Goshe from the Department of Molecular and Structural Biochemistry at NC State for their support in ligand development and proteomics development. They would additionally like to acknowledge David C. Muddiman, Allison Stewart, and the Molecular Education, Technology and Research Innovation Center (METRIC) for time and equipment used in support of proteomics efforts. Lastly, they would like to acknowledge their funding and support for this project through the William R. Kenan, Jr. Institute for Engineering, Technology & Science.

ORCID

R. Ashton Lavoie http://orcid.org/0000-0001-9842-8520

REFERENCES

Aboulaich, N., Chung, W. K., Thompson, J. H., Larkin, C., Robbins, D., & Zhu, M. (2014). A novel approach to monitor clearance of host cell proteins associated with monoclonal antibodies. *Biotechnology Progress*, *30*, 1114–1124.

Bailey-Kellogg, C., Gutiérrez, A. H., Moise, L., Terry, F., Martin, W. D., & De Groot, A. S. (2014). CHOPPI: A web tool for the analysis of immunogenicity risk from host cell proteins in CHO-based protein production. *Biotechnology and Bioengineering*, *111*, 2170–2182.

Bee, J. S., Tie, L., Johnson, D., Dimitrova, M. N., Jusino, K. C., & Afdahl, C. D. (2015). Trace levels of the CHO host cell protease cathepsin D caused particle formation in a monoclonal antibody product. *Biotechnology Progress*, *31*, 1360–1369.

Chiu, J., Valente, K. N., Levy, N. E., Min, L., Lenhoff, A. M., & Lee, K. H. (2017). Knockout of a difficult-to-remove CHO host cell protein, lipoprotein lipase, for improved polysorbate stability in monoclonal antibody formulations. *Biotechnology and Bioengineering*, *114*, 1006–1015.

Cooper, B., Feng, J., & Garrett, W. M. (2010). Relative, label-free protein quantitation: Spectral counting error statistics from nine replicate MudPIT samples. *Journal of the American Society for Mass Spectrometry*, *21*, 1534–1546. https://doi.org/10.1016/j.jasms.2010.05.001

Fischer, S. K., Cheu, M., Peng, K., Lowe, J., Araujo, J., Murray, E., … Song, A. (2017). Specific immune response to phospholipase B-like 2 protein, a host cell impurity in lebrikizumab clinical material. *AAPS Journal*, *19*, 254–263. http://link.springer.com/10.1208/s12248-016-9998-7

Fuchs, S. GRAVY Calculator. http://www.gravy-calculator.de/index.php

Gagnon, P., Nian, R., Lee, J., Tan, L., Latiff, S. M. A., Lim, C. L., … Gan, H. T. (2014). Nonspecific interactions of chromatin with immunoglobulin G and protein A, and their impact on purification performance. *Journal of Chromatography A*, *1340*, 68–78. https://doi.org/10.1016/j.chroma.2014.03.010

Gan, H. T., Lee, J., Latiff, S. M. A., Chuah, C., Toh, P., Lee, W. Y., & Gagnon, P. (2013). Characterization and removal of aggregates formed by nonspecific interaction of IgM monoclonal antibodies with chromatin catabolites during cell culture production. *Journal of Chromatography A*, *1291*, 33–40. http://www.ncbi.nlm.nih.gov/pubmed/23598159

Gilgunn, S., El-sabbahy, H., Albrecht, S., Gaikwad, M., Corrigan, K., Deakin, L., … Bones, J. (2019). Identification and tracking of problematic host cell proteins removed by a synthetic, highly functionalized nonwoven media in downstream bioprocessing of monoclonal antibodies. *Journal of Chromatography A*, *1595*, 28–38. https://doi.org/10.1016/j.chroma.2019.02.056

Goey, C. H., Alhuthali, S., & Kontoravdi, C. (2018). Host cell protein removal from biopharmaceutical preparations: Towards the implementation of quality by design. *Biotechnology Advances*, *36*, 1223–1237. https://doi.org/10.1016/j.biotechadv.2018.03.021

Hogwood, C. E. M., Tait, A. S., Koloteva-Levine, N., Bracewell, D. G., & Smales, C. M. (2013). The dynamics of the CHO host cell protein profile during clarification and protein A capture in a platform antibody purification process. *Biotechnology and Bioengineering*, *110*, 240–251.

Jawa, V., Joubert, M. K., Zhang, Q., Deshpande, M., Hapuarachchi, S., Hall, M. P., & Flynn, G. C. (2016). Evaluating immunogenicity risk due to host cell protein impurities in antibody-based biotherapeutics. *AAPS Journal*, *18*, 1439–1452. http://link.springer.com/10.1208/s12248-016-9948-4

Kornecki, M., Mestmäcker, F., Zobel-Roos, S., Heikaus de Figueiredo, L., Schlüter, H., & Strube, J. (2017). Host cell proteins in biologics manufacturing: The good, the bad, and the ugly. *Antibodies*, *6*, 1–18.

Kyte, J, Doolittle, RF, Diego, S, & Jolla, L. (1982). A simple method for displaying the hydropathic character of a protein. *Journal of Molecular Biology*, *157*(1), 105–1032.

Lavoie, R. A., di Fazio, A., Blackburn, R. K., Goshe, M., Carbonell, R. G., & Menegatti, S. (2019). Targeted capture of Chinese hamster ovary host cell proteins: Peptide ligand discovery. *International Journal of Molecular Sciences*, *20*, 1729. https://www.mdpi.com/1422-0067/20/7/1729

Levy, N. E., Valente, K. N., Choe, L. H., Lee, K. H., & Lenhoff, A. M. (2014). Identification and characterization of host cell protein product-

associated impurities in monoclonal antibody bioprocessing. *Biotechnology and Bioengineering*, *111*, 904–912.

Mechetner, L., Sood, R., Nguyen, V., Gagnon, P., & Parseghian, M. H. (2011). The effects of hitchhiker antigens co-eluting with affinity-purified research antibodies. *Journal of Chromatography B*, *879*, 2583–2594.

Menegatti, S., Bobay, B. G., Ward, K. L., Islam, T., Kish, W. S., Naik, A. D., & Carbonell, R. G. (2016). Design of protease-resistant peptide ligands for the purification of antibodies from human plasma. *Journal of Chromatography A*, *1445*, 93–104. https://doi.org/10.1016/j.chroma.2016.03.087

Neilson, K. A., Keighley, T., Pascovici, D., Cooke, B., & Haynes, P. (2013). Label-free quantitative shotgun proteomics using normalized spectral abundance factors. In M.Zhou, & T.Veenstra (Eds.), *Proteomics Biomark. Discov. Methods Protoc* (1002, pp. 205–222). Springer Science+Business Media.

Park, J. H., Jin, J. H., Lim, M. S., An, H. J., Kim, J. W., & Lee, G. M. (2017). Proteomic analysis of host cell protein dynamics in the culture supernatants of antibody-producing CHO cells. *Scientific Reports*, *7*, 1–13. https://doi.org/10.1038/srep44246

Singh, N., Arunkumar, A., Peck, M., Voloshin, A. M., Moreno, A. M., Tan, Z., …Li, Z. J. (2017). Development of adsorptive hybrid filters to enable two-step purification of biologics. *mAbs*, *9*, 350–363.

Swiss Institute of Bioinformatics. Compute MW/pI. *ExPasy Bioinforma. Resour. Portal*. http://web.expasy.org/compute_pi/

Tsumoto, K, Ejima, D, Senczuk, AM, Kita, Y, & Arakawa, T. (2007). Effects of salts on protein-surface interactions: Applications for column chromatography. *Journal of Pharmaceutical Sciences*, *96*(7), 1677–1690.

Valente, K. N., Lenhoff, A. M., & Lee, K. H. (2015). Expression of difficult-to-remove host cell protein impurities during extended Chinese hamster ovary cell culture and their impact on continuous bioprocessing. *Biotechnology and Bioengineering*, *112*, 1232–1242.

Wisniewski, J. R., Zougman, A., Nagaraj, N., & Mann, M. (2009). Universal sample preparation method for proteome analysis. *Nature Methods*, *6*, 359–363.

Zhang, Q., Goetze, A. M., Cui, H., Wylie, J., Trimble, S., Hewig, A., & Flynn, G. C. (2014). Comprehensive tracking of host cell proteins during monoclonal antibody purifications using mass spectrometry Comprehensive tracking of host cell proteins during monoclonal antibody purifications using mass spectrometry. *mAbs*, *6*, 659–670.

Zhang, Q., Goetze, A. M., Cui, H., Wylie, J., Tillotson, B., Hewig, A., … Flynn, G. C. (2016). Characterization of the co-elution of host cell proteins with monoclonal antibodies during protein A purification. *Biotechnology Progress*, *32*, 708–717.

SUPPORTING INFORMATION

Additional supporting information may be found online in the Supporting Information section.

How to cite this article: Lavoie RA, di Fazio A, Williams TI, Carbonell R, Menegatti S. Targeted capture of Chinese hamster ovary host cell proteins: Peptide ligand binding by proteomic analysis. *Biotechnology and Bioengineering*. 2020;117:438–452. https://doi.org/10.1002/bit.27213